Monte Carlo-based Reliability Estimation Methods for Power Devices in Power Electronics Systems

Novak, Mateja; Sangwongwanich, Ariya; Blaabjerg, Frede

Published in:
IEEE Open Journal of Power Electronics

DOI (link to publication from Publisher):
10.1109/OJPEL.2021.3116070

Publication date:
2021

Document Version
Publisher's PDF, also known as Version of record

IEEE Open Journal of
Power Electronics

Received 13 August 2021; revised 14 September 2021; accepted 20 September 2021. Date of publication 28 September 2021; date of current version 15 October 2021. The review of this article was arranged by Associate Editor Shu Yang.

Digital Object Identifier 10.1109/OJPEL.2021.3116070

Monte Carlo-Based Reliability Estimation Methods for Power Devices in Power Electronics Systems

M. NOVAK (Member, IEEE), A. SANGWONGWANICH (Member, IEEE), AND F. BLAABJERG (Fellow, IEEE)

AAU Energy, Aalborg University, Aalborg 9200, Denmark

CORRESPONDING AUTHOR: MATEJA NOVAK (e-mail: nov@energy.aau.dk).

The work is supported by the Reliable Power Electronic-Based Power System (REPEPS) project at the AAU Energy, Aalborg University as a part of the Villum Investigator Program funded by the Villum Foundation.

ABSTRACT Monte Carlo simulation has been widely used for reliability assessment of power electronic systems. In this approach, multiple simulations are carried out during the lifetime estimation of the components in power converter, e.g., power devices, where the parameter variations are considered. In the previous mission-profile based reliability assessment methods, the dynamic thermal stress profiles are usually converted into a set of static parameters. However, this simplification may introduce a certain uncertainty during the reliability assessment, since the static parameters may not be able to accurately represent the thermal stress under highly dynamic conditions. Moreover, the previous research did not take into account the correlation between the method of introducing the parameter variation and the required number of Monte Carlo simulations. This can significantly affect both the accuracy and computation burden of the Monte Carlo simulation. To address this issue, an in-depth analysis of Monte Carlo simulation applied to reliability assessment of power devices in power electronic systems is provided in this paper. Two additional Monte Carlo simulation approaches based on semi-dynamic and dynamic parameters are proposed, and their reliability evaluation results are compared with the traditional static parameter method. It is demonstrated in a case study of photovoltaic (PV) inverter application that the reliability of power converter can be overestimated up to 30% when using the static parameters.

INDEX TERMS Power converter, reliability, lifetime prediction, mission profiles, Monte Carlo methods.

I. INTRODUCTION

Power electronic systems play an important role in enabling power conversion and control in several applications such as automotive, power supplies, and renewable energy systems [1]. In many of these applications, a failure of power electronic systems can compromise the safety of user or system operator (e.g., in automotive applications) [2], while for the less safety-critical applications, the unexpected failure will trigger an unscheduled maintenance and give lower system availability, which can significantly increase the cost [3], e.g., in renewable energy applications. Therefore, reliability is an aspect that needs to be taken into consideration during the design of power electronic systems, where the reliability assessment method plays a crucial part [4].

There has been a paradigm shift in the reliability assessment of power electronic systems, where physics-of-failure becomes more relevant [5]–[7]. On the other hand, the handbook-based approach (e.g., MIL-HDBK-217F [8]) is considered to be outdated [9], since its assumption of constant failure rate is no longer representing the majority of failures in real operation of modern power electronic systems. In power electronic systems, power semiconductor devices are considered as reliability-critical components (together with electrolytic capacitors), which are responsible for a majority of failures in field-operation [2]. The degradation of the power devices are mainly caused by the thermal stress. In the early studies, the reliability assessment of power devices in power electronics usually relies on an empirical lifetime model [10], which is applied to the intended operating conditions, referred to as mission profiles [11], [12]. The outcome of this approach is a deterministic estimation of failure rate (e.g., number of cycle-to-failure or time-to-failure). Later on, the reliability

prediction method has been improved by including the stochastic behaviour of the model parameters [7], in order to take into account the uncertainty in the prediction due to parameter variations, e.g., tolerance during manufacturing process [13]. In that case, the reliability performance of the power converter is represented by a probability of failure (which usually increases over time due to the component's ageing/wear-out) with a certain distribution rather than a deterministic value.

It is very common to use Monte Carlo simulations for analysing stochastic behaviour of model parameters, which represents uncertainty in the prediction [14]. Monte Carlo method relies on multiple simulations (also called experiments), where the model parameters are modelled with a certain distribution, representing the variation, and they are randomly selected during each simulation [15]. Then, based on the law of large numbers [14], it is expected that the simulation results will converge to the expected value, if the number of simulations is large enough. In that case, the result of the Monte Carlo method (with a large number of simulations) will be a distribution, which provides the information about the probability of each possible outcome. In other words, when applying this method to the reliability prediction, the probability of failure rate over time (e.g., during the entire operation) can be determined.

In the previous research, the Monte Carlo simulations have been applied for the reliability assessment of power electronics in several applications. The original idea has been applied to the reliability prediction of PV inverters in [16], and the same approach has been followed by the others [17]–[22]. This method has also been extended to the power converters used in wind turbines [23], motor drives [24], [25], power supplies [26]–[28], and electric aircraft [29] applications. However, the previous research fails to provide a guideline to select an appropriate number of simulations when applying the Monte Carlo method to the reliability assessment of power electronic systems. According to most of the previous work, a "rule of thumb" of 10 000 simulations (as it was first introduced in [16]) is assumed to be large enough to ensure that the results are converging, regardless of the parameter variation range (e.g., uncertainty). Only a few publications use different number of simulations (e.g., 1000 [30], 5000 [22], and 100 000 [20]), but the argument of the parameter choice is still missing. The number of required simulations is an important factor in the Monte Carlo method, which affects both the accuracy and the computational burden of the entire process [14]. While using an extremely large number of simulations can almost certainly ensure the convergence of the results, it can slow down the simulation significantly, which amplifies the drawback of Monte Carlo simulation approach. This factor can be critical when being applied in an optimization routine during the design of power converters.

Moreover, in the previous work the dynamic stress parameters are usually converted to an equivalent static one during the Monte Carlo simulation, as it was proposed in [16]. This approach is simple and can effectively calculate the lifetime distribution by applying a variation to the static values in Monte Carlo simulations. However, for a very high dynamic mission profile, e.g., due to load variations, a simple representation of all the dynamics of a power device junction temperature with one set of static parameters may introduce a certain error. It has been demonstrated in [31] that different implementation methods of Monte Carlo simulation can also affect the modelling accuracy. However, a guideline for selecting a suitable number of simulations for each method has not been discussed. Thus, there is a lack of systematic approach to select the Monte Carlo simulation parameters, e.g., the required number of simulations, which limits its application in the reliability prediction of power electronics.

In order to address the above issue, this paper, which is an extension of the authors' previous work in [31], aims to provide an in-depth analysis of Monte Carlo simulation-based reliability assessment method for power electronic systems. Compared to [31], where different methods of implementing parameter variations were presented on two application cases, the analysis in this paper is extended with a comprehensive guideline for parameter selection of Monte Carlo simulation to determine the minimum required number of simulation for a given parameter variation condition, and thereby minimize the computational burden of the analysis. It is based on a case study of PV inverter system, whose system configuration is provided in Section II. In Section III workflow of the mission profile-based reliability assessment of power devices in PV inverter is given. Different implementation methods of Monte Carlo simulation for the application of reliability prediction in power electronic devices are discussed in Section IV, where two alternative approaches are proposed in additional to the conventional one. The performance of all three Monte Carlo simulation methods under different parameter variation ranges is compared in terms of modelling accuracy and computational efficiency. Afterwards, the influence of the Monte Carlo methods on the thermal stress and end-of-life distribution is analyzed in Section V. Then, a guideline for selection of the suitable number of simulation for each Monte Carlo simulation method is provided in Section VI. Finally, concluding remarks are summarized in Section VII.

II. SYSTEM CONFIGURATION

In this paper, the Monte Carlo-based reliability assessment methods are applied to a case study of power devices in PV inverters. The system configuration of PV inverter in PV-standalone application is shown in Fig. 1, where the two-level three-phase inverter is employed to extract the power from the PV array with the maximum power point tracking (MPPT) operation implemented. The extracted dc-power is then converted to the ac-power and supply the load. The overall system parameters are summarized in Table 1, while the physical hardware prototype is shown in Fig. 2. To emulate the behaviour of a PV array, the test bench uses a PV simulator. Optic fiber is attached to the centre of the chip surface of the power device as shown in Fig. 2. The junction temperature

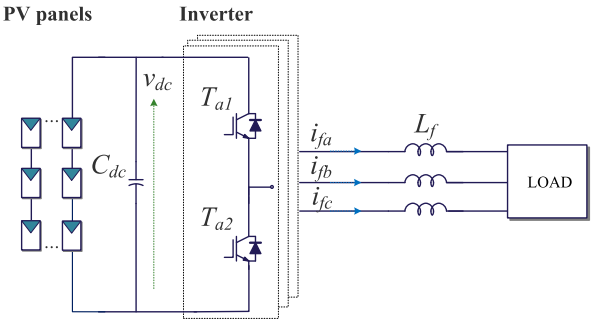

FIGURE 1. System configuration of two-level three-phase inverter in a standalone PV application.

TABLE 1. Parameters of the Three-Phase PV Inverter

PV array rated power	2500 W
Output current (rated)	i_f = 30 A
DC-link voltage	v_{dc} = 400-600 V
DC-link capacitance	C_{dc} = 340 μF
Filter inductance	L = 2.5 mH
Resistive load	R = 16.5 Ω
Switching frequency	f_{sw} = 10 kHz
Nominal output frequency	f_g = 50 Hz

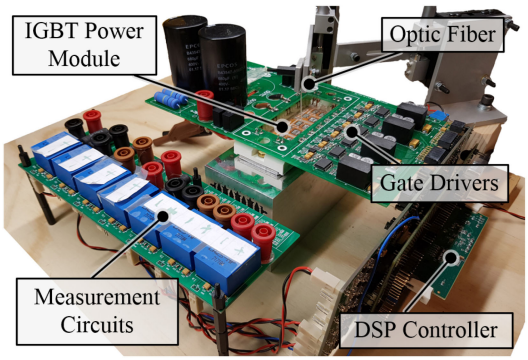

FIGURE 2. PV inverter test-bench used for obtaining the power device thermal stress profile.

from the opened module [32] is measured and recorded using the signal conditioner.

Clearly, the operating condition of the PV inverter, referred to as mission profile, is strongly dependent on the environmental conditions of the PV arrays (e.g., solar irradiance and ambient temperature). An example of one-day mission profile during clear-day and cloudy-day conditions is demonstrated in Fig. 3. It is therefore important to model the power losses and thermal stress conditions of the power devices in the PV inverter during the entire operation in order to apply the lifetime analysis discussed in the following section.

A. POWER LOSSES MODELING

A 1200 V/50 A Insulated-Gate Bipolar Transistors (IGBTs) module [32] is used as the power devices in the inverter prototype. The power loss characteristics of the power devices (e.g., conduction and switching losses) are modelled by using the datasheet parameters, as it is given in Fig. 4. For instance, the

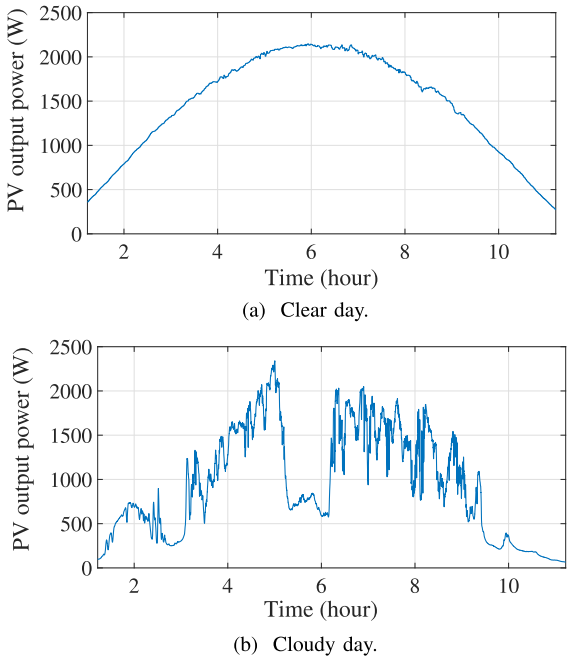

FIGURE 3. Power production (mission profile) of the PV system during: a) a clear day and b) a cloudy day.

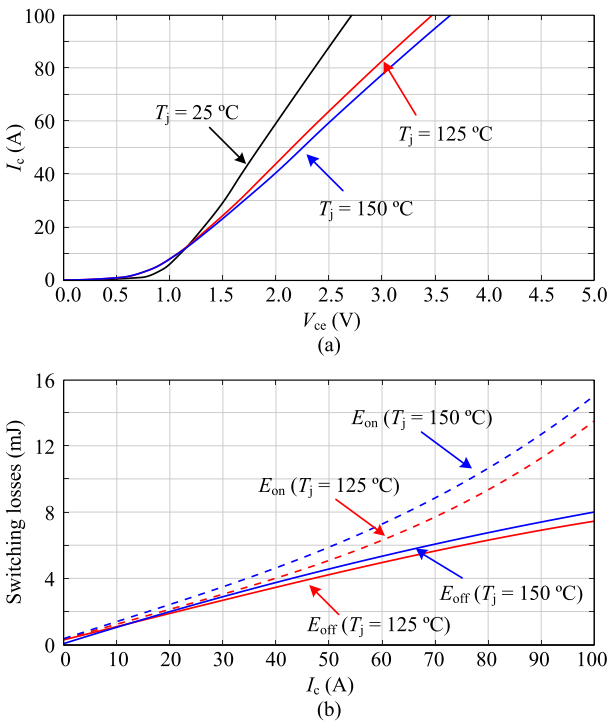

FIGURE 4. Power loss characteristic of the IGBT: a) Output characteristic (V_{ce} is the on-state collector-emitter voltage) and b) Switching losses (E_{on} and E_{off} are the energy loss during turn-on and turn-off, respectively) [32].

conduction loss can be obtained from the output characteristic of the power device in Fig. 4(a), while the switching losses can be obtained from the energy loss during the turn-on and turn-off as it is shown in Fig. 4(b).

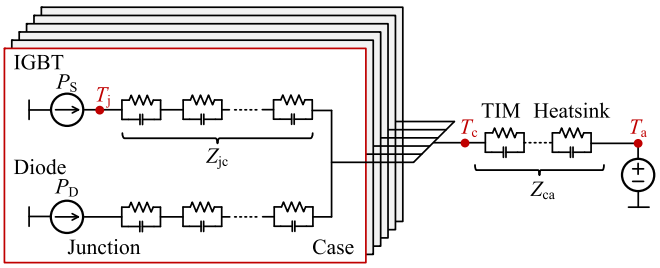

FIGURE 5. Thermal impedance of the three-phase IGBT module base on Foster's thermal network (TIM: thermal interface material).

TABLE 2. Parameters of the Thermal Impedance Z_{jc} and Z_{ca} [32]

Layer i	1	2	3	4
Thermal resistance $R_{jc,i}$	0.0324	0.1782	0.1728	0.1566
Thermal capacitance $C_{jc,i}$	0.3086	0.1122	0.2894	0.6386
Thermal resistance $R_{ca,i}$	0.0670	0.1737	0.0869	-
Thermal capacitance $C_{ca,i}$	6,157	404.72	37.335	-

To enable a long-term simulation (e.g., daily operation), the power losses model is implemented as a look-up table, which gives a good compromise between the accuracy and computational burden. The same approach is also applied to the power losses modeling of the anti-parallel diode, and thus will not be repeated here. A comprehensive power losses calculation method can be found in [33].

B. THERMAL STRESS MODELING

A thermal model is required in order to estimate the thermal stress, e.g., junction temperature, of the power device under certain operating conditions. The thermal model of the three-phase IGBT module used in PV inverter is shown in Fig. 5. The thermal network is based on the Foster's model, whose parameters can be fitted from the experimental results (which is the case in this paper), and therefore has been widely applied in practical applications.

The thermal impedance in Fig. 5 can be divided into two parts: 1) junction-to-case Z_{jc} and 2) case-to-ambient Z_{ca}. The junction-to-case thermal impedance Z_{jc} contributes to the temperature rise of each individual device (e.g., IGBT and diode) when the power loss is generated. Then, the thermal impedances of all the devices are coupled at the case (since they all share the same case and heatsink), where the case-to-ambient thermal impedance Z_{ca} contributes to the temperature rise of the case due to the total power losses of all the devices in the power module. The parameters of the thermal impedance network are summarized in Table 2. The overall junction temperature of the IGBT can be calculated as

$$T_j = P_S \cdot Z_{jc} + 6 \cdot (P_S + P_D) \cdot Z_{ca} + T_a \tag{1}$$

where T_a is the ambient temperature, P_S and P_D are the total power losses of the IGBT and diode, discussed in the previous section. The accuracy of the modelling has already been validated in [34]. Thus, it will not be repeated here.

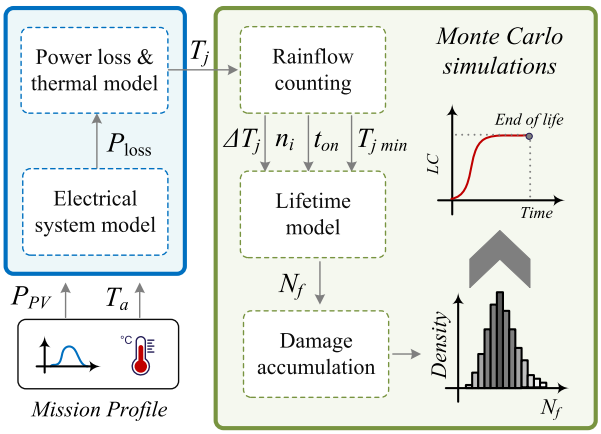

FIGURE 6. Workflow of the mission-profile based reliability assessment of power devices.

III. LIFETIME EVALUATION OF POWER DEVICES

As shown in the lifetime evaluation workflow in Fig. 6, the first step is the stress analysis of the power devices. The outcome of the analysis is a thermal stress profile of the power devices for a given mission profile, which is an input of the whole modelling process. In the next step, the obtained thermal stress profile is applied to the lifetime model. Depending on the selected lifetime model [35], specific parameters of the thermal cycles need to be obtained at this step by using a cycle counting algorithm. These parameters are used afterwards to calculate the lifetime consumption of the power devices. In the final step, Monte Carlo simulations are applied to include the variations in the stress and lifetime model parameters.

A. MISSION PROFILE TRANSLATION TO THERMAL LOADING

The stress conditions are related to the mission profile of the power devices (e.g. voltages, currents, and ambient temperature) and they are reflected in the junction temperature variation of the power devices during the operation. This is typically obtained by using an electro-thermal model of the power converter system. For the PV inverter, the mission profile is defined by the input power obtained from the PV panels (P_{PV}) and the ambient temperature (T_a). The power losses in the power devices and the heatsink will cause junction temperature fluctuations. By using the thermal model of the power devices introduced in Section II-B with power losses and ambient temperature as input variables, the junction temperature profile (T_j) of the devices can be obtained. As mentioned earlier, this process is implemented as a look-up table to provide a fast estimation of junction temperature profile under a long-term mission profile.

B. THERMAL CYCLE COUNTING

The thermal cycling occurs in the junction temperature of the power devices and it is the main cause of wear-out failure in the power device. Thus, the thermal cycling information needs to be obtained from the junction temperature profile, which

TABLE 3. Lifetime Model Parameters of IGBT Module [10]

Parameter	Value	Parameter	Value
A	$9.34 \cdot 10^{14}$	β_2	1285
I_B	12.5	β_3	-0.463
V_C	12	β_4	-0.716
D	300	β_5	-0.761
β_1	-4.416	β_6	-0.5

contains variation introduced by the ambient temperature and loading conditions. It is required to employ a cycle counting algorithm like Rainflow algorithm to identify the thermal cycles, and group the thermal cycles by the cycle period, the cycle amplitude, and the mean value. For the selected lifetime model, the algorithm is used to obtain the number of cycles n_i, temperature swing ΔT_j, minimum junction temperature $T_{j,min}$, and heating time t_{on} from the junction temperature profile [7], [35].

C. ESTIMATION OF THE LIFETIME CONSUMPTION

The empirical lifetime model is used to predict the number of cycles to failure (N_f) under a certain thermal stress conditions. The lifetime model of the IGBT module is typically obtained from the power cycling test results, where the most widely used lifetime model of the power devices is given in the following [10]:

$$N_f = A \cdot \Delta T_j^{\beta_1} \exp\left(\frac{\beta_2}{T_{j,min} + 273}\right) \cdot t_{on}^{\beta_3} \cdot I_B^{\beta_4} \cdot V_C^{\beta_5} \cdot D^{\beta_6} \tag{2}$$

where $\beta_1, \beta_2, \ldots, \beta_6$ are the model fitting parameters, A is the technology factor parameter, I_B is the value of the current per bond wire, D is the bond wire diameter and V_c is the voltage class of the module. The parameter values used in this paper are summarized in Table 3.

After obtaining the number of cycles to failure, the Lifetime Consumption (LC) of the power device can be calculated using the Miner's rule as in (3) [35] :

$$LC = \sum_i \frac{n_i}{N_{fi}} \tag{3}$$

where n_i is the number of cycles and N_{fi} is the number of cycles to failure for the same cycle and stress condition calculated from (2).

IV. MONTE CARLO SIMULATION METHODS

As discussed earlier, parameter variations are normally introduced during the lifetime estimation by Monte Carlo simulation. For an empirical lifetime model in (2), there are several model parameters that may introduce uncertainty. For the model fitting parameters (β_1, β_2,..., β_6), the interval of variance is already given in [10]. On the other hand, the thermal stress parameters (e.g., junction temperature) will also vary to a certain range in practice. Generally, a certain distribution type (e.g., normal distribution) with its variation range can be applied to represent the variation in the thermal stress parameters [16]. For instance, the manufacturer usually provide the typical values and the maximum (or minimum) value of the power device's characteristics which can differ from the nominal value [32], [36] and these parameters can introduce variation in the junction temperature of the devices even when the same mission profile is being applied. To simplify the presented approach, in this paper the parameter variability trough the time, e.g., due to degradation, was not considered. To take this aspect into account the change in the structure of the device, an accurate physics-based electrical device model is required as shown in [37]. Here, both parasitic electrical elements and thermal impedance network are extracted from the finite-element analysis of the module geometry. The accurate model and thermal network are used to obtain an offline mapping of power losses and thermal behaviour of the devices. However, this approach demands heavy computation effort, especially during Monte Carlo simulation, and therefore where not considered in this work. Moreover, it was found out in [37] that the consumed lifetime during the PV mission profile was not strongly affect by the impact of parameter degradation, i.e., the increased loss is less than 1%. Nevertheless, the degradation may need to be considered when applying longer or more severe loading to the device.

There are different approaches to implement Monte Carlo simulation for the reliability assessment, which will affect the results. In this paper, the three following approaches will be considered:

- Monte Carlo with static parameters **(MC-SP)**
- Monte Carlo with semi-dynamic parameters **(MC-SDP)**
- Monte Carlo with dynamic parameters **(MC-DP)**

A. MONTE CARLO WITH STATIC PARAMETERS (MC-SP)

The Monte Carlo using static parameters (MC-SP) is a conventional method for reliability assessment of the power devices, which was proposed in [16]. It requires a conversion of the dynamic thermal stress profile to an equivalent set of static parameters. In the first step, the dynamic thermal stress profile is applied to the lifetime model (2) in order to obtain a lifetime consumption (LC_{dyn}). Afterwards, using the same lifetime model, a set of static stress parameters (ΔT_j, t_{on} and $T_{j\,min}$) that will result in the same lifetime consumption LC_{dyn} value are calculated. To reduce the degree of freedom, it is suggested to calculate $t_{on\,static}$ and $T_{j\,min\,static}$ from the average values of the dynamic t_{on} and $T_{j\,min}$. Thus, the remaining variable in (2) is $\Delta T_{j\,static}$ which can be calculated analytically. After obtaining these static parameters, a variation with normal distribution $var(m)$ is applied to the parameters $\Delta T_{j\,static}$ and $T_{j\,min\,static}$ as it is shown in Fig 7(a).

The distribution of $\Delta T_{j\,MC-SP}$ when using the MC-SP method can be obtained as:

$$\Delta T_{j\,MC-SP}(m) = \Delta T_{j\,static} + var(m) \cdot \Delta T_{j\,static} \tag{4}$$

where m is the number of Monte Carlo simulations that will be conducted. In the next step, the static $\Delta T_{j\,MC-SP}$ and $T_{j\,min\,MC-SP}$ distributions are sampled during each simulation

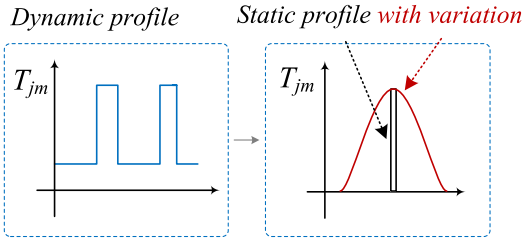

(a) Monte Carlo with static parameters.

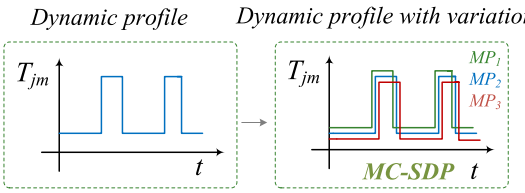

(b) Monte Carlo with semi-dynamic parameters.

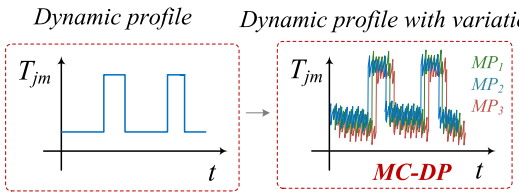

(c) Monte Carlo with dynamic parameters.

FIGURE 7. Monte Carlo simulation methods based on: a) static parameters (MC-SP), b) semi-dynamic parameters (MC-SDP), and c) dynamic parameters (MC-DP).

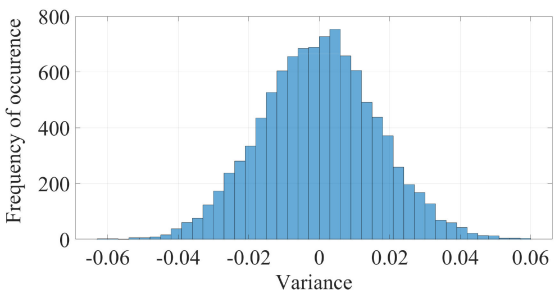

FIGURE 8. Example of a normal distribution with 5% variance.

for calculating the distribution of the lifetime consumption (LC), which takes into account the parameter variations.

B. MONTE CARLO WITH SEMI-DYNAMIC PARAMETERS (MC-SDP)

The Monte Carlo analysis with semi-dynamic parameters (MC-SDP) is proposed in this paper, whose modeling principle is as follows. During each Monte Carlo simulation, one sample is randomly picked from the variance distribution (e.g. from a 5% variance shown in Fig. 8) and the variation range from this sample is then applied to the entire dynamic profile. As demonstrated in the example from Fig. 7(b) after conducting three Monte Carlo simulations, the original dynamic profile $T_{j\,orig}(t)$ is transformed into multiple dynamic profiles (MP_1, MP_2, MP_3) where each dynamic profile has a fixed variance var_1, var_2, var_3 that has been sampled from the normal distribution $var(m)$. Thus, the thermal stress profile when applying the Monte Carlo simulations with semi-dynamic parameter can be obtained as:

$$T_{j\,MC-SDP}(m,t) = T_{j\,orig}(t) + var(m) \cdot T_{j\,orig}(t) \quad (5)$$

where m is the number of Monte Carlo simulations and t is the number of samples in the thermal stress profile for each simulation. In other words, each Monte Carlo simulation with semi-dynamic parameters has a different variance, however the variance is constant during the whole thermal stress profile of one Monte Carlo simulation. Compared to the MC-SP, the MC-SDP method does not require a conversion of the dynamic profile to the static profile when applying parameter variation. However, this approach will increase the required number of calculations/simulations and thereby results in a higher computational burden compared to the MC-SP method.

C. MONTE CARLO WITH DYNAMIC PARAMETERS (MC-DP)

Another Monte Carlo method proposed in this paper is based on dynamic parameters (MC-DP). In this method, the parameter variation is applied to the dynamic thermal stress profile in the following way. For each Monte Carlo simulation, the parameter variation is randomly chosen (e.g., from a normal distribution like presented in Fig. 8) for each sample during the entire process. Thus, the parameter variation range that is being applied during one Monte Carlo simulation will not be constant (like the MC-SDP method), but dynamically change over time (or samples in discrete time-domain). Therefore, the thermal stress profiles obtained from the MC-DP method can be derived as:

$$T_{j\,MC-DP}(m,t) = T_{j\,orig}(t) + var(m,t) \cdot T_{j\,orig}(t) \quad (6)$$

where m is the number of Monte Carlo simulations that will be conducted and t is the number of samples in the thermal stress profile for each simulation. It is worth to mention that the variation $var(m,t)$ is time-dependent in this case. The process is then repeated for all m Monte Carlo simulations. In this way, all the samples of one dynamic mission profile do not have a constant variance like in MC-SDP. In Fig. 7(c) it can be observed how the introduced variation transforms the original dynamic mission profile into three new dynamic profiles (MP_1, MP_2, MP_3). Compared to the other Monte Carlo simulation methods, the MC-DP is a truly stochastic approach, but it requires the highest computational effort since it is introducing the parameter variation sample-by-sample. A summary of the characteristics of three Monte Carlo methods is given in Table. 4.

V. RELIABILITY ASSESSMENT OF POWER ELECTRONICS BASED ON MONTE CARLO SIMULATIONS

In this section, the reliability assessment of PV inverter based on the three Monte Carlo simulation methods will be discussed following the workflow in Fig. 6.

TABLE 4. Comparison of the Monte Carlo Simulation Methods

MC method	Stress profile	Variance	Total no. of calculations
MC-SP	Time independent	Time independent	m
MC-SDP	Time dependent	Time independent	$m * t$
MC-DP	Time dependent	Time dependent	$m * t * t$

Note: m is number of MC simulations, t is number of stress profile samples

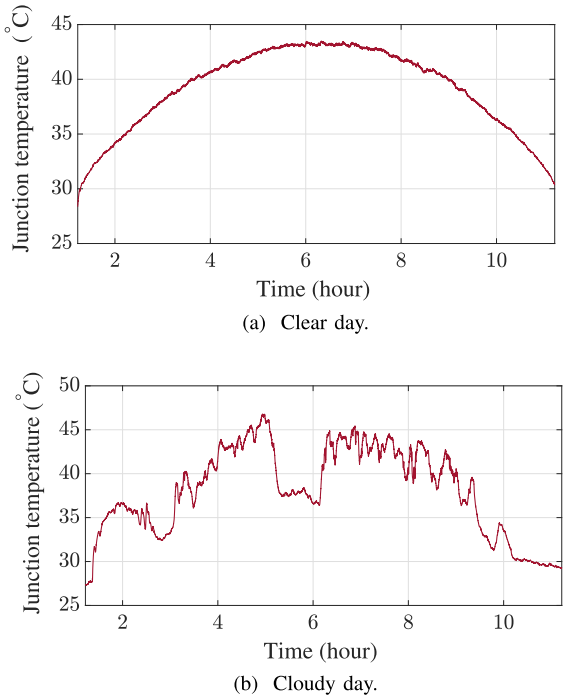

FIGURE 9. Junction temperature profiles obtained from the PV inverter test-bench for input power shown in Fig. 3.

A. THERMAL STRESS ANALYSIS

The original thermal stress profile of the power device was obtained from the two-level PV inverter in the test-bench shown in Fig. 2. In the experiments, a PV simulator was programmed to emulate the behavior of the PV array during a clear day (see Fig. 3(a)) and also during a cloudy day (see Fig. 3(b)). The corresponding power device junction temperatures can be observed in Fig. 9 for both operating conditions. For the cloudy day, the fluctuation in the energy production from the PV array will cause high temperature swings. In the conventional Monte Carlo simulation based on static parameters, these thermal stress profiles will be converted into a set of static parameters (e.g., ΔT_j, t_{on}, and $T_{j\,min}$), which provides equivalent lifetime consumption as when applying the original thermal stress profile.

In order to apply the MC-SDP method, a constant variation needs to be applied to the thermal stress profile in Fig. 9. An example of the obtained thermal stress profile when a constant variation of 2% and 5% are applied to the original thermal stress profile (represented by the case with parameter variation of 0%) is shown in Fig. 10. It can be observed from the results

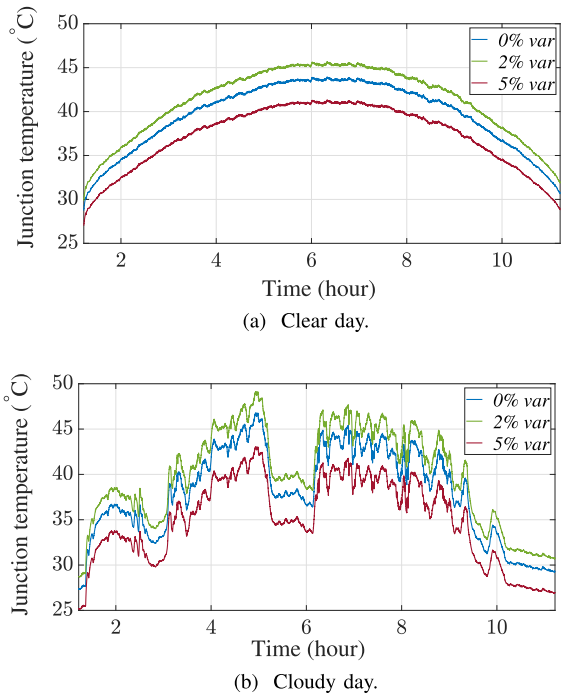

FIGURE 10. Dynamic junction temperature profiles in Monte Carlo method with semi-dynamic parameters (MC-SDP).

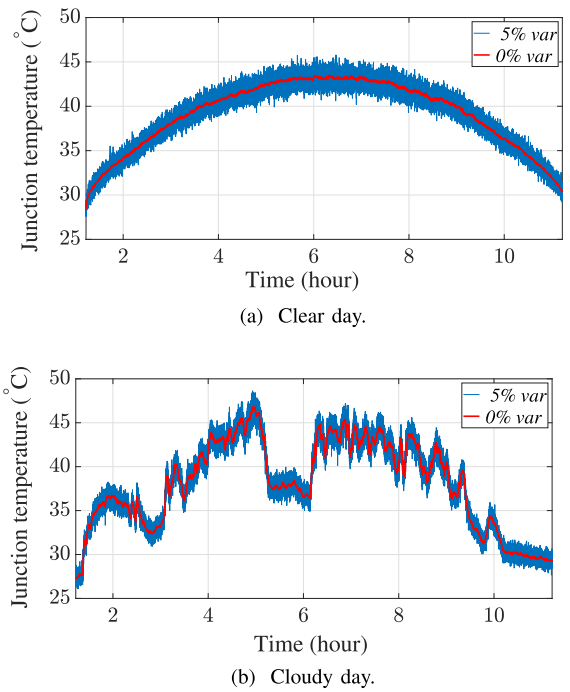

FIGURE 11. Dynamic junction temperature profile in Monte Carlo method with dynamic parameters (MC-DP).

that for all three Monte Carlo simulations, the variation in the thermal stress profile is kept the same during each simulation.

On the other hand, when using the MC-DP method, a dynamic parameter variation needs to be applied to the thermal stress profile during each Monte Carlo simulation, instead of a fixed value. This process is demonstrated in Fig. 11, where

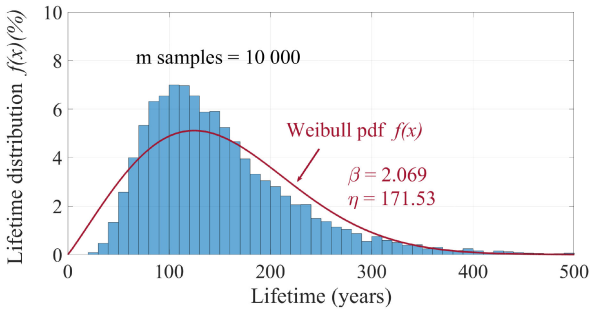

FIGURE 12. Lifetime distribution of one power device of the PV inverter using MC-DP with parameter variation of 5%.

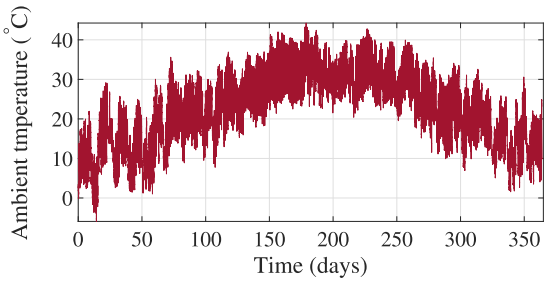

(a) Ambient temperature.

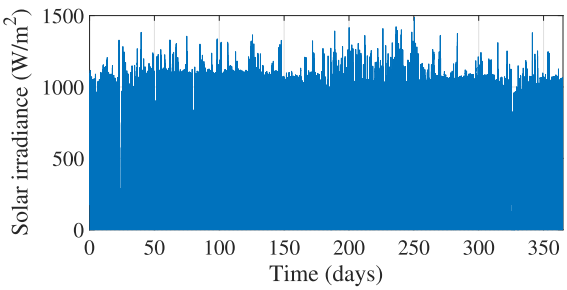

(b) Solar irradiance.

FIGURE 13. Yearly mission profile used for end-of-life estimation of the PV inverter.

a dynamic parameter variation based on a normal distribution with standard deviation of 5% is applied. It can be seen that the thermal stress profile obtained from the MC-DP method is highly stochastic compared to the previous two methods, since the variation is applied randomly sample-by-sample.

B. END-OF-LIFE DISTRIBUTION ANALYSIS

The end-of-life analysis will be performed using a yearly mission profile of solar irradiance and ambient temperature measurements in Arizona, shown in Fig. 13.

When applying the thermal stress profiles (or static parameters) obtained from the Monte Carlo simulations to the lifetime model introduced in (2), a lifetime distribution of the samples used in the Monte Carlo simulations can be obtained. The lifetime distribution of the power devices typically follows the shape of Weibull distribution as shown in Fig. 12. The presented approach can also be applied to other distributions. The Weibull distribution is chosen as an example as it is one of the most widely used distributions to represent the wear-out failure of power components in power electronics industry, especially for the lifetime model obtained from power cycling. This can also be observed in following power cycling reports [38]–[41]. The distribution can therefore be fitted by the Weibull probability density function (*pdf*):

$$f(x) = \frac{\beta}{\eta^{\beta}} x^{\beta-1} exp\left[-\left(\frac{x}{\eta}\right)^{\beta} \right] \tag{7}$$

where η is the scale parameter and β is the shape parameter. η also corresponds to the time when 63.2% of the population have failed and β parameter defines the failure mode. $\beta > 1$ implies increasing failure rate and it is related with the wear-out leading to end-of-life of the component [14].

To obtain the end-of-life cumulative distribution function (*cdf*), i.e. the unreliability function for the power devices, the *pdf* function needs to be integrated. In this way a number of the failed devices in the population at the time x can be obtained:

$$F(x) = \int_0^x f(x)dx \tag{8}$$

After obtaining the unreliability functions for a single power device, the system-level unreliability function $F_{sys}(x)$, which represent the entire power module of the two-level PV inverter (i.e., 6 IGBTs), can be calculated as:

$$F_{sys}(x) = 1 - (1 - F_{T_1}(x))^6 \tag{9}$$

where $F_{T_1}(x)$ is the unreliability function of a single power device in the two-level inverter. It is assumed that the loading conditions in each phase are equal, which is typically the case for three-phase inverter. Therefore, the unreliability functions of the $F_{T_1}(x)$ can be raised to the power of 6 in order to obtain the system-level unreliability function $F_{sys}(x)$. Due to unidirectional power flow and unity power factor requirement of the PV application in this paper, the diodes are not experiencing high thermal loading like the IGBT devices. Therefore, the analysis is simplified to only include the IGBT devices, which significantly contribute to the lifetime consumption of the inverter.

A population of 10 000 simulations was used in the three Monte Carlo simulation methods. Among the three methods, the MC-SP method can achieve the fastest calculation time, while the MC-DP method is the slowest due to its large number of calculations. To illustrate the execution time, the MC-SP method was executed in 1 s, which had a thermal stress profile of almost 104 000 samples (in discrete time-domain). The MC-SDP method required 100 seconds and MC-DP method required 160 seconds to achieve the same number of samples. The differences in the execution time among different Monte Carlo simulation methods indicate the computation efficiency of different approaches, as it has been discussed in Table 4, where the MC-DP method has the highest computational burden compared to the other approaches.

The reliability of power devices in PV inverter is carried out using three different Monte Carlo simulation methods. In

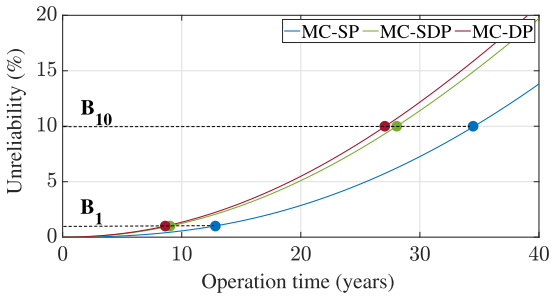

FIGURE 14. Comparison of unreliability functions when using Monte Carlo simulation with static parameters (MC-SP) and semi-dynamic parameters (MC-SDP), and dynamic parameters (MC-DP) with parameter variation of 1%.

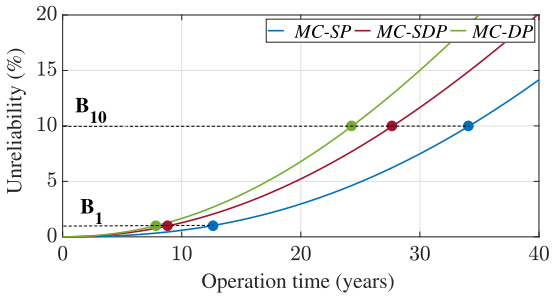

FIGURE 15. Comparison of unreliability functions when using Monte Carlo simulation with static parameters (MC-SP) and semi-dynamic parameters (MC-SDP), and dynamic parameters (MC-DP) with parameter variation of 5%.

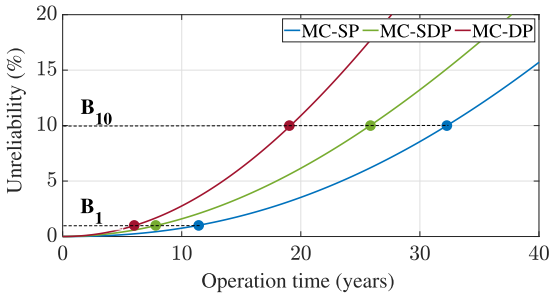

FIGURE 16. Comparison of unreliability functions when using Monte Carlo simulation with static parameters (MC-SP) and semi-dynamic parameters (MC-SDP), and dynamic parameters (MC-DP) with parameter variation of 10%.

Fig. 14, the unreliability functions for the PV inverter with parameter variation of 1% can be observed. The unreliability functions of the MC-DP method show a significantly different results than the MC-SP method. If the lifetime model parameter variation is increased to 5% and 10% a difference in the unreliability curve of different Monte Carlo methods (e.g., the MC-DP and MC-SDP methods) is more pronounced as it can be observed in Fig. 15 and Fig. 16, respectively. The MC-SP method results in the longest expected lifetime, while the MC-DP method estimates the shortest in all three evaluated cases.

One of the commonly used metrics in the lifetime analysis is the B_x lifetime i.e. the time when x% of the device population have failed. In Figs. 14-16, B_1 and B_{10} lifetime, are

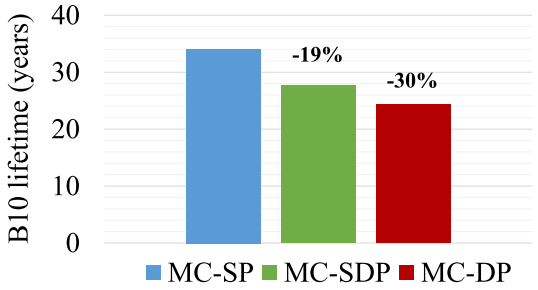

FIGURE 17. B_{10} lifetime for the PV inverter obtained from different Monte Carlo simulation methods with parameter variation of 5%.

highlighted. The expected B_1 and B_{10} lifetimes for all cases are summarized in Table 5. When comparing the B_{10} lifetimes obtained from the MC-SP and the MC-SDP methods, the difference is around 18%. In the comparison to the MC-DP method, this difference is even larger as shown in Fig. 17. It can also be observed that different values of parameter variation don't have a high impact on the B_1 and B_{10} lifetimes when MC-SP is used, compared to MC-DP where depending on the parameter variance the results can differ up to 30% for the presented case application if 1% or 10% variance is used. This is due to the fact that parameter variance in MC-SP is added after the analysis of the thermal cycles, thus it does not influence in large extend the parameters of the thermal cycles that were used to calculate the accumulated damage.

VI. PARAMETER SELECTION GUIDELINE FOR MONTE CARLO SIMULATIONS

One of the aspects that needs to be carefully considered for all three Monte Carlo simulation methods is the selection of parameter during the analysis. Since the Monte Carlo simulation approach requires multiple simulations, the accuracy of the analysis relies heavily on the number of simulation. If insufficient number of simulations is used, the estimated values of the outcome from Monte Carlo simulation will not converge. In other words, the reliability evaluation results will not be repeatable even when applying the same thermal stress conditions, and the metrics such as B_{10} and B_1 lifetime will not provide a meaningful information. Therefore, it is crucial to ensure that the number of simulation used in the Monte Carlo analysis is large enough. However, employing too large number of simulation will increase the computational burden significantly, while the improvement in the modeling accuracy is very limited, which should be avoided. Therefore, it is crucial to provide a guideline for selecting a suitable number of simulations for different Monte Carlo simulation methods.

A. RESULTS EVALUATION

In order to identify a suitable number of simulation, different number of simulations of 100, 1000, 10 000, and 100 000 Monte Carlo simulations are employed for all three Monte Carlo simulation methods (e.g., MC-SP, MC-SDP, and MC-DP). For each Monte Carlo simulation method, three parameter variation ranges of 1%, 5%, and 10% are used. This

TABLE 5. B_1 and B_{10} Lifetime Estimation (years) for Different Parameter Variations in Monte Carlo Simulations

MC simulation methods	MC-SP			MC-SDP			MC-DP		
Parameter variation	1%	5%	10%	1%	5%	10%	1%	5%	10%
B_1	12.83	12.63	11.42	9.02	8.81	7.82	8.62	7.82	6.01
B_{10}	34.47	34.07	32.26	28.06	27.65	25.85	27.05	24.25	19.04

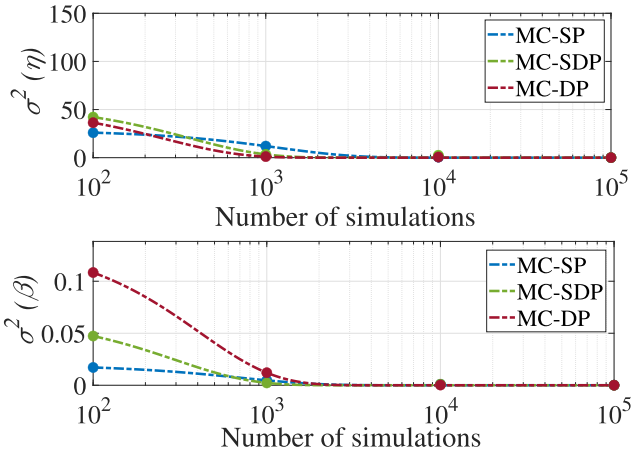

FIGURE 18. Dependence of variance (σ) of the Weibull distribution parameters (η, β) and number of simulations in the three Monte Carlo simulation methods when the parameter variation is 1%.

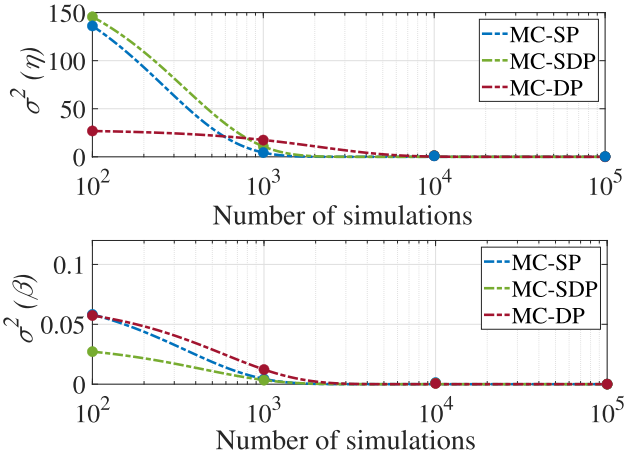

FIGURE 19. Dependence of variance (σ) of the Weibull distribution parameters (η, β)and number of simulations in the three Monte Carlo simulation methods when the parameter variation is 5%.

process is repeated 5 times (for each number of simulation case, parameter variation range, and Monte Carlo simulation method), in order to observe the convergence of the results.

Two parameters that define the Weibull lifetime distribution, which are the outcome of Monte Carlo simulation methods, are the scale parameter (η) and shape parameter (β). The variance/standard deviation (σ) of these two parameters will be used for benchmarking the convergence of the Monte Carlo simulation methods, and they can be calculated from:

$$\sigma^2(x) = \frac{\sum_{n=1}^{N}((x_n - \bar{x})^2)}{N-1}, x \in [\eta, \beta] \qquad (10)$$

where N is set to 5 (since the process is repeated 5 times) and $\bar{x}$ is the mean value.

In Fig. 18, the results are presented for the three Monte Carlo simulation methods where the variance of the parameters variation of 1% is considered. It can be observed that the scale parameter η has a larger variance than the shape parameter β, as it is expected, since β indicates the failure mechanism. Low variance of β confirms that the failure mechanism for the three Monte Carlo simulation methods remains the same. The figure also shows that a low number of simulations (100) does not lead to convergence of the scale parameter. For MC-SP method, the required number of simulation is 10 000, while the MC-SDP and MC-DP methods show good convergence already when the number of simulation is 1000.

If the parameter variation range is increased to 5%, all three Monte Carlo simulation methods reach the convergence when the number of simulation is around 10 000, as it shown in Fig. 19. It is interesting to notice that the MC-DP method has

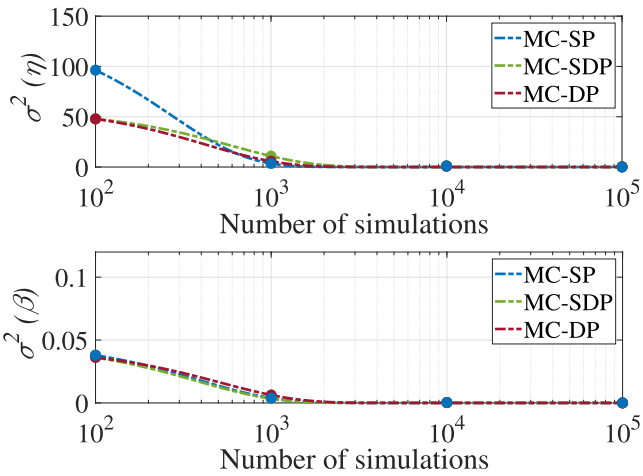

FIGURE 20. Dependence of variance (σ) of the Weibull distribution parameters (η and β) and number of simulations in the three Monte Carlo simulation methods when the parameter variation is 10%.

a much lower variance than MC-SP and MC-SDP methods even for 100 simulations. For the last case, when the model parameter variation is increased to 10%, all three Monte Carlo simulation methods reach the convergence at already 1000 simulations, as it shown in Fig. 20. Only a small reduction of the variance is visible for the case with 10 000 simulations.

B. SELECTION OF NUMBER OF SIMULATIONS

Overall, if all the obtained results are considered, it can be concluded that a minimum number of 1000 simulations can provide the convergence of the Weibull lifetime distribution

for the three Monte Carlo simulation methods applied to the reliability assessment of the PV inverter in this case study. Applying a higher number of simulation will significantly improve the model accuracy, while the computational burden will increase considerably. This is applicable for all variation ranges (e.g., 1%, 5%, and 10%). It was also noticed that the convergence is much faster for the small variation range of the model parameter (e.g., 1%). However, when a lower number of simulations is used, the convergence of the reliability evaluation results is not guarantee, as it is highly dependent on the applied Monte Carlo method.

C. SELECTION OF MONTE CARLO METHODS

In general, the differences in the Weibull parameters (i.e., η and β) among different Monte Carlo simulation methods are not significant once the results are converged. This is applied to the case when the number of simulation is above 1000 simulations. However, the selection of Monte Carlo methods becomes more important with the low number of simulations (e.g., 100). It can be observed from the results in Figs. 18–20 that the MC-DP method generally provide a more accurate result, where the Weibull parameters are close to the expected value (and thus their variances are small). This is mainly due to the true stochastic nature of this Monte Carlo implementation approach. Thus, for a low number of simulations, it is recommended to used the MC-DP for the reliability analysis. Moreover, the computational burden is usually not a major concern in such low number of simulation condition.

VII. CONCLUSION

A comparison of three different Monte Carlo simulation methods used for reliability assessment of power electronic converters is presented in this paper. The use of conventional Monte Carlo simulation with static parameters provides a fast calculation of lifetime distribution, but the error in the estimated B_{10} lifetime can be as high as 30% compared to the other Monte Carlo simulation methods with more dynamic parameter variation. Therefore, a certain design margin may needs to be allocated if the Monte Carlo simulation with static parameters are used in the reliability assessment of the power converter. Moreover, the guideline for selecting the required number of simulations for all three Monte Carlo simulation methods has been carried out in this paper. It has been demonstrated with a case study of PV inverter that the reliability assessment results generally converge when the number of simulation reaches 1000, which is ten times lower than the typical number of simulation used in the previous study. Moreover, when a low number of simulation is used (e.g., 100), the Monte Carlo method based on the dynamic parameters is more suitable to be applied due to its smaller deviation in the results compared to the other approaches. Thus, the outcome of this analysis provides a more systematical way to evaluate and select a suitable number of simulations for Monte Carlo simulation methods, ensuring a high modelling accuracy while at the same time minimize the computation burden.

REFERENCES

[1] F. Blaabjerg, Z. Chen, and S. B. Kjaer, "Power electronics as efficient interface in dispersed power generation systems," *IEEE Trans. Power Electron.*, vol. 19, no. 5, pp. 1184–1194, Sep. 2004.

[2] Y. Song and B. Wang, "Survey on reliability of power electronic systems," *IEEE Trans. Power Electron.*, vol. 28, no. 1, pp. 591–604, Jan. 2013.

[3] G. Petrone, G. Spagnuolo, R. Teodorescu, M. Veerachary, and M. Vitelli, "Reliability issues in photovoltaic power processing systems," *IEEE Trans. Ind. Electron.*, vol. 55, no. 7, pp. 2569–2580, Jul. 2008.

[4] H. Wang, K. Ma, and F. Blaabjerg, "Design for reliability of power electronic systems," in *Proc. IECON*, 2012, pp. 33–44.

[5] H. Wang, M. Liserre, and F. Blaabjerg, "Toward reliable power electronics: Challenges, design tools, and opportunities," *IEEE Ind. Electron. Mag.*, vol. 7, no. 2, pp. 17–26, Jun. 2013.

[6] H. Wang *et al.*, "Transitioning to physics-of-failure as a reliability driver in power electronics," *IEEE J. Emerg. Sel. Topics Power Electron.*, vol. 2, no. 1, pp. 97–114, Mar. 2014.

[7] K. Ma, H. Wang, and F. Blaabjerg, "New approaches to reliability assessment: Using physics-of-failure for prediction and design in power electronics systems," *IEEE Power Electron. Mag.*, vol. 3, no. 4, pp. 28–41, Dec. 2016.

[8] U. S. Department of Defense, "Reliability prediction of electronic equipment," U. S. Department of Defense, Tech. Rep. MIL-HDBK-217F/2, Washington, DC, USA, 1991.

[9] E. De Francesco, R. De Francesco, and E. Petritoli, "Obsolescence of the MIL-HDBK-217: A critical review," in *Proc. MetroAeroSpace*, 2017, pp. 282–286.

[10] R. Bayerer, T. Herrmann, T. Licht, J. Lutz, and M. Feller, "Model for power cycling lifetime of IGBT modules - various factors influencing lifetime," in *Proc. 5th Int. Conf. Integrated Power Electron. Syst.*, 2008, pp. 1–6.

[11] H. Huang and P. A. Mawby, "A lifetime estimation technique for voltage source inverters," *IEEE Trans. Power Electron.*, vol. 28, no. 8, pp. 4113–4119, Aug. 2013.

[12] M. Musallam, C. Yin, C. Bailey, and M. Johnson, "Mission profile-based reliability design and real-time life consumption estimation in power electronics," *IEEE Trans. Power Electron.*, vol. 30, no. 5, pp. 2601–2613, May 2015.

[13] R. Spence and R. Soin, *Tolerance Design of Electronic Circuits, Ser. Electronic Systems Engineering Series*. Wokingham, UK: Addison-Wesley, 1988.

[14] P. O'Connor and A. Kleyner, *Practical Reliability Engineering*. Hoboken, NJ, USA: Wiley, 2012.

[15] A. Alghassi, S. Perinpanayagam, M. Samie, and T. Sreenuch, "Computationally efficient, real-time, and embeddable prognostic techniques for power electronics," *IEEE Trans. Power Electron.*, vol. 30, no. 5, pp. 2623–2634, May 2015.

[16] P. D. Reigosa, H. Wang, Y. Yang, and F. Blaabjerg, "Prediction of bond wire fatigue of IGBTs in a PV inverter under a long-term operation," *IEEE Trans. Power Electron.*, vol. 31, no. 10, pp. 7171–7182, Oct. 2016.

[17] Y. Yang, A. Sangwongwanich, and F. Blaabjerg, "Design for reliability of power electronics for grid-connected photovoltaic systems," *CPSS Trans. Power Electron. Appl.*, vol. 1, no. 1, pp. 92–103, 2016.

[18] A. Sangwongwanich, Y. Yang, D. Sera, and F. Blaabjerg, "Lifetime evaluation of grid-connected PV inverters considering panel degradation rates and installation sites," *IEEE Trans. Power Electron.*, vol. 33, no. 2, pp. 1225–1236, Feb. 2018.

[19] A. Sangwongwanich, Y. Yang, D. Sera, F. Blaabjerg, and D. Zhou, "On the impacts of PV array sizing on the inverter reliability and lifetime," *IEEE Trans. Ind. App.*, vol. 54, no. 4, pp. 3656–3667, Jul./Aug. 2018.

[20] Y. Shen, A. Chub, H. Wang, D. Vinnikov, E. Liivik, and F. Blaabjerg, "Wear-out failure analysis of an impedance-source PV microinverter based on system-level electrothermal modeling," *IEEE Trans. Ind. Electron.*, vol. 66, no. 5, pp. 3914–3927, May 2019.

[21] J. He, A. Sangwongwanich, Y. Yang, and F. Iannuzzo, "Lifetime evaluation of three-level inverters for 1500-V photovoltaic systems," *IEEE J. Emerg. Sel. Topics Power Electron.*, vol. 9, no. 4, pp. 4285–4298, Aug. 2021.

[22] J. M. S. Callegari, A. F. Cupertino, V. d. N. Ferreira, and H. A. Pereira, "Minimum DC-link voltage control for efficiency and reliability improvement in PV inverters," *IEEE Trans. Power Electron.*, vol. 36, no. 5, pp. 5512–5520, May 2021.

[23] D. Zhou, G. Zhang, and F. Blaabjerg, "Optimal selection of power converter in DFIG wind turbine with enhanced system-level reliability," *IEEE Trans. Ind. App.*, vol. 54, no. 4, pp. 3637–3644, Jul./Aug. 2018.
[24] A. Soldati, G. Pietrini, M. Dalboni, and C. Concari, "Electric-vehicle power converters model-based design-for-reliability," *CPSS Trans. Power Electron. Appl.*, vol. 3, no. 2, pp. 102–110, 2018.
[25] I. Vernica, H. Wang, and F. Blaabjerg, "Design for reliability and robustness tool platform for power electronic systems - study case on motor drive applications," in *Proc. IEEE Appl. Power Electron. Conf. Expo.*, 2018, pp. 1799–1806.
[26] D. Zhou, H. Wang, and F. Blaabjerg, "Mission profile based system-level reliability analysis of DC/DC converters for a backup power application," *IEEE Tran. Power Electron.*, vol. 33, no. 9, pp. 8030–8039, Sep. 2018.
[27] M. Novak, V. Ferreira, M. Andresen, T. Dragicevic, F. Blaabjerg, and M. Liserre, "FS-MPC based thermal stress balancing and reliability analysis for NPC converters," *IEEE Open J. Power Electron.*, vol. 2, pp. 124–137, Feb. 2021.
[28] V. Ferreira, M. Andresen, B. Cardoso, and M. Liserre, "Pulse-shadowing-based thermal balancing in multichip modules," *IEEE Trans. Ind. App.*, vol. 56, no. 4, pp. 4081–4088, Jul./Aug. 2020.
[29] V. Raveendran, M. Andresen, and M. Liserre, "Improving onboard converter reliability for more electric aircraft with lifetime-based control," *IEEE Trans. Ind. Electron.*, vol. 66, no. 7, pp. 5787–5796, Jul. 2019.
[30] C. Lv, J. Liu, Y. Zhang, W. Lei, R. Cao, and G. Lv, "Reliability modeling for metallized film capacitors based on time-varying stress mission profile and aging of ESR," *IEEE J. Emerg. Sel. Topics Power Electron.*, vol. 9, no. 4, pp. 4311–4319, Aug. 2021.
[31] M. Novak, A. Sangwongwanich, and F. Blaabjerg, "Monte Carlo based reliability estimation methods in power electronics," in *Proc. IEEE 21st Workshop Control Model. Power Electron.*, 2020, pp. 1–7.
[32] Infineon Technologies AG, "FS50R12KT4 B15 datasheet," Nov. 2013, rev. 3.0.
[33] Infineon Technologies AG, "IGBT Power Losses Calculation Using the Data-Sheet Parameters," Jan. 2009, rev. 1.1.
[34] A. Sangwongwanich, Y. Yang, D. Sera, and F. Blaabjerg, "Mission profile-oriented control for reliability and lifetime of photovoltaic inverters," *IEEE Trans. Ind. Appl.*, vol. 56, no. 1, pp. 601–610, Jan. 2020.
[35] Z. Ni *et al.*, "Overview of real-time lifetime prediction and extension for SiC power converters," *IEEE Trans. Power Electron.*, vol. 35, no. 8, pp. 7765–7794, Aug. 2020.
[36] Semikron, "SKiiP 28MlI07E3V1 datasheet", Jun. 2016, rev. 1.0.
[37] L. Ceccarelli, R. M. Kotecha, A. S. Bahman, F. Iannuzzo, and H. A. Mantooth, "Mission-profile-based lifetime prediction for a SiC MOSFET power module using a multi-step condition-mapping simulation strategy," *IEEE Trans. Power Electron.*, vol. 34, no. 10, pp. 9698–9708, Oct. 2019.
[38] U. Choi, S. Jorgensen, F. Iannuzzo, and F. Blaabjerg, "Power cycling test of transfer molded IGBT modules by advanced power cycler under different junction temperature swings," *Microelectronics Rel.*, vol. 88–90, pp. 788–794, 2018.
[39] J. Lutz, C. Schwabe, G. Zeng, and L. Hein, "Validity of power cycling lifetime models for modules and extension to low temperature swings," in *Proc. EPE'20 ECCE Europe*, 2020, pp. 1–9.
[40] N. Kaminski, "Application Note 5SYA 2043-04: Load-cycling capability of HiPak IGBT modules," ABB Switzerland Ltd Semiconductors, pp.1–8, Feb. 2014, rev. 4.0.
[41] L. Borucki, T. Kimmer, O. Schilling, and G. Zeng, "How long is your system going to last?," *Bodo's Power Syst.*, vol. pp. 32–34, Dec. 2018.